Optical properties of Tm^{3+}-doped photonic crystal fiber fabricated by non-chemical vapor deposition method

CHANGMING XIA[a,*] GUIYAO ZHOU[a,b], WEI ZHANG[a], YING HAN[b], CHAO WANG[b], JINHUI YUAN[a]
[a]*Guangdong Province Key Laboratory of Nano-photonic Functional Materials and Devices, South China Normal University, Guangzhou, 510006, China*
[b]*State Key Laboratory of Metastable Materials Science & Technology, Yanshan University, Qinhuangdao, 066004, China*

In this paper, the Tm^{3+}-doped photonic crystal fiber (PCF) is fabricated by non-chemical vapor deposition method (NCVD) for the first time. The absorption, fluorescence, and attenuation properties of Tm^{3+}-doped PCF are experimentally investigated. The results show that the Tm^{3+}-doped PCF has the potential application on the high power fiber laser.

(Received December 19, 2013; accepted May 7, 2015)

Keywords: Tm^{3+}-doped photonic crystal fiber, Non-chemical vapor deposition method (NCVD), Optical properties

1. Introduction

In recent years, the fiber lasers have attracted increased attentions because they can provide the excellent beam quality, compact system configuration, easy thermal management, and high optical efficiency [1, 2]. At present, the fiber laser has achieved the power output of kW near 1 μm spectral region using the Yb^{3+}-doped silica fiber [3]. However, the high power fiber lasers in the mid-infrared region around 2 μm fabricated by Tm^{3+} doped, Ho^{3+} doped, and Tm^{3+}/ Ho^{3+} co-doped glasses, have been a new substantial interest due to its widely potential applications on the infrared-guided missile countermeasure, optical communications, remote sensing, material processing, and medicine [4-8]. In addition, they can be used as the pump source for the generation of mid-infrared light by nonlinear effects [9-11]. Compared with the Yb^{3+}-doped fiber laser, the spectral range of Tm^{3+}-doped fiber laser can be tunable from 1850 to 2200 nm. Because of the cross-relaxation energy transfer between thulium ions in the Tm^{3+} doped fiber laser, the quantum efficiency near 2 can be obtained for the thulium ions $^3F_4 \rightarrow {}^3H_6$ transition when the Tm^{3+}-doped concentration is enough highly. The simplified energy-level diagram of Tm^{3+} ions in silica glass is shown in Fig. 1. In the transfer process of the cross-relaxation energy ($^3H_6$, $^3H_4 \rightarrow {}^3F_4$, $^3F_4$), two ground-level thulium ions can be excited to the upper lasing level of the $^3F_4 \rightarrow {}^3H_6$ transition by absorbing only one 790 nm pump photon, which means one excited Tm^{3+} ion at the level of $^3H_4$ generates two Tm^{3+} ions at the level of $^3F_4$ upper laser. Thus, the thulium exhibits a unique feature that the slope efficiency can exceed the Stokes limit, that is to say that the thulium-doped silica fiber lasers can achieve the theoretical slope efficiency of 80% [12].

In 2009, Clarkson et al. demonstrated the slope efficiency of 70% in the Tm^{3+}-doped fiber laser [13]. At present, the Tm^{3+}-doped fiber laser has achieved the kW output power [14]. However, some properties of Tm-doped fiber limit the development of high power Tm-doped fiber laser, such as the nonlinear effect, quantum defect heating, up-conversion effect, and photo-darkening, and so on. Using the diode laser as the pump source, Norbert et al firstly demonstrated a novel Tm^{3+}-doped photonic crystal fiber (PCF) laser with the CW output power of 4W, the slope efficiency of 36.6%, and M^2<1.25, but the effect of quantum defect heating needed to be considered [15]. In 2012, Pankaj et al demonstrated a novel ultra-large mode field area Tm-doped PCF laser with the peak power of 6.5 KW, the diffraction-limited beam quality, and the high polarization purity [16]. Using the Tm-doped PCF rod as the gain media, Gaida et al carried out the CW laser and amplification experiment, and achieved the laser output of 20 W using the diode laser with 793 nm as the pump source [17]. In above reports, all of active media are the Tm-doped fiber fabricated by the modified chemical vapor deposition (MCVD) and the solution doping process [18, 19]. In this paper, we show the fabrication of Tm^{3+}-doped photonic crystal fiber based on the non-chemical vapor deposition method (NCVD) for the first time. Compared to the conventional CVD, this method has the superior control of the homogeneity and accuracy of doping concentrations, which can be applicable to the multi-rare earth co-doping, large core, and high concentration configurations to aid the development of high power fiber lasers.

2. Experiment

The fabrication process of Tm^{3+}-doped PCF perform includes two phases. One is preparation of the Tm^{3+} doped silica glass for the Tm^{3+}-doped PCF perform core, another is the preparation of Tm^{3+}-doped PCF perform. In the first phase, the core rod of preform is fabricated by combining the high temperature plasma furnace sintering technology with the dry granulated oxides. The fabrication process of dry granulated oxides can be divided into three steps.

Step 1, the $TmCl_3$ and $AlCl_3$ solution are accurately mixed according to the weight fraction.

Step 2, $SiCl_4$ is added into the solution of $TmCl_3$ and $AlCl_3$ by a carrier gas of O_2. The reaction of $SiCl_4$, $TmCl_3$, and $AlCl_3$ with H_2O can form the Sol-Gel-like material in solution under the temperature of 60℃. In the material science, the Sol-Gel process is a method for producing the solid materials from small molecules used for the fabrication of metal oxides [20].

Step 3, the mixed powder is obtained after drying the superfluous water. To eliminate OH^-, the mixed powder is heated at the temperature of 1000 ℃ with the atmosphere of O_2 and Cl_2. Then the dry granulated oxides with low OH^- are obtained. The composition of dry granulated oxides is SiO_2, Tm_2O_3, and Al_2O_3.

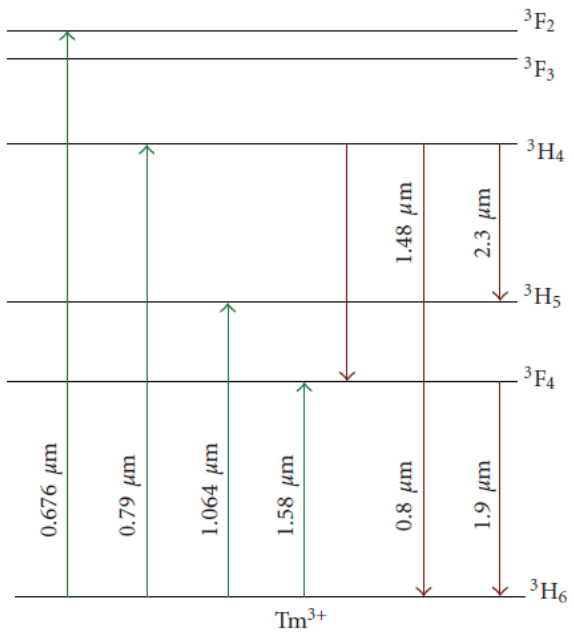

Fig. 1. The simplified energy-level diagram of Tm^{3+} ions in silica glass.

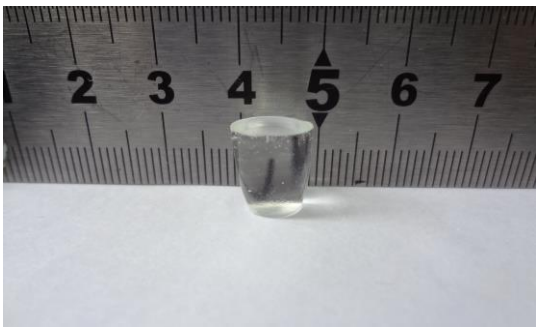

Fig. 2. The sample rod of Tm^{3+}-doped silica rod fabricated by NCVD.

Then, the dry granulated oxides is brought into the high temperature plasma furnace (the furnace temperature is near 3000 ℃) to vitrify by a carrier gas of O_2. Finally, the Tm^{3+}-doped silica rods with no bubbles are successfully fabricated. Thereafter, the Tm^{3+} doped silica glass rod is prepared by milling and polishing to use for the core rod of PCF preform. The sample is shown in Fig. 2, where the diameter of Tm^{3+} doped silica glass rod is about 10 mm.

In the second phase, the Tm^{3+} doped PCF perform is prepared by the stack capillaries method. The core capillaries of PCF perform are replaced using the Tm^{3+}-doped silica glass rod, and the Tm^{3+}-doped PCF perform is successfully fabricated.

Then the Tm^{3+}-doped PCF perform is drawn into the fiber under the high temperature of 2000 ℃. The cross-section of the dual-cladding Tm^{3+}-doped PCF fabricated by the NCVD method is shown in Fig. 4.

3. Results and discussion

The absorption spectrum of Tm^{3+}-doped silica glass rod in the visible and infrared regions at the room temperature is shown in Fig. 3. The absorption spectra of the developed glass are recorded through Ocean Optics's Maya 2000-Pro and NIRQuest 256 2.5 spectrophotometer for 200~2500 nm using the tungsten halogen lamp as the light source. As seen from the Fig. 3, a strong absorption band centered at 790 nm is observed, corresponding to the $^3H_6 \rightarrow {}^3H_4$ transition of Tm^{3+}. In addition, an intensive wide band at 1630 nm is also observed, which is ascribed to the $^3H_6 \rightarrow {}^3F_4$ transition of Tm^{3+}. The wide absorption band indicates that the silica glass fabricated by the NCVD method can be efficiently excited by LD around 1630 nm.

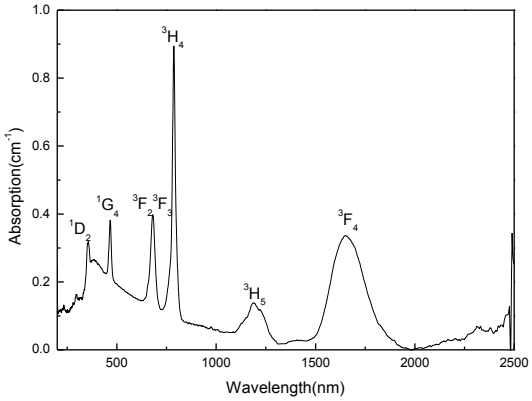

Fig. 3. Absorption spectrum of Tm^{3+}-doped silica rod fabricated by NCVD.

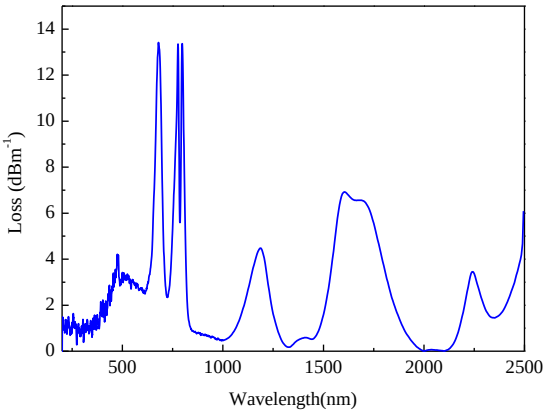

Fig. 5. The attenuation spectrum of Tm^{3+}-doped photonic crystal fiber.

Fig. 4 shows the cross-section of dual-cladding Tm^{3+}-doped silica PCF. As seen from Fig. 4, the outer cladding of PCF is disorder because of the hot expansion effect of the capillaries in the outer cladding region. The PCF has a hole size to pitch (d/Λ) ratio of 0.19 with a pitch of 11.97 μm. The silica glass core with 50 μm diameter is doped with 1.0 wt% Tm and co-doped with Al (the ratio of Tm/Al is 1:8).

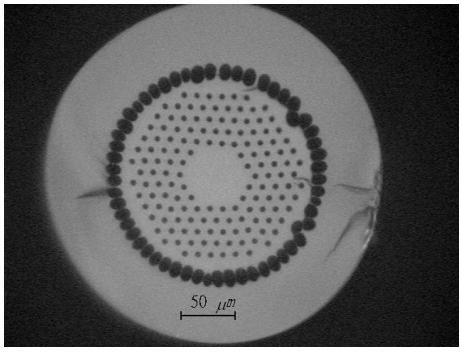

Fig. 4. The cross-section of Tm^{3+}-doped photonic crystal fiber fabrication by NCVD.

The cut back method is implemented to determine fiber attenuation. Fig. 5 shows the attenuation spectrum of Tm^{3+}-doped silica PCF in the range of 200 to 2500 nm. As shown in Fig. 5, the absorption attenuation at 793 nm ($^3H_6 \rightarrow {}^3F_4$) is 10.413 dBm^{-1} (the attenuation at 790 nm of NKT's Tm^{3+}-doped PCF with 2.5% Tm is ~17 dBm^{-1}), 13.415 dBm^{-1} at 680 nm for energy leve1 $^3H_6 \rightarrow {}^3F_2/{}^3F_3$ transition, 4.479 dBm^{-1} at 1185 nm for energy level $^3H_6 \rightarrow {}^3H_5$ transition, 6.919 dBm^{-1}at 1605 nm for energy leve1 $^3H_6 \rightarrow {}^3F_4$ transition, and 0.001 dBm^{-1} at 2000 nm. In addition, the absorption attenuation bandwidth around 1605 nm is up to 255 nm, which offer a good condition for pumping the Tm^{3+}-doped silica PCF using the infrared diode laser around 1750 nm as the pump source.

Fig. 6 shows the NIR fluorescence spectrum in the range of 900 to 2500 nm of the Tm^{3+} doped PCF. In the experiment, the length of PCF is 1 m. An intense and broad emission band centered at 2170 nm is observed, corresponding to the $^3F_4 \rightarrow {}^3H_6$ transition of Tm^{3+}. It is interesting that the fluorescence peak of 2170 nm in the Tm^{3+}-doped PCF with NCVD method is longer than that by CVD method, which is longer than the emission peak of Ho^{3+}-doped silica fiber [21]. According to our analysis, the fluorescence peak centered at 2170 nm is also within the laser wavelength of Tm^{3+}-doped silica fiber [22]. However, because of the high background loss of the fiber around 2000 nm, it is difficult to observe the fluorescence peak longer than 2100 nm in the silica fiber with CVD method. This phenomenon shows that the background loss around 2100 nm of the Tm^{3+}-doped PCF fabricated with NCVD method is very low, as seen from Fig. 5. As shown in Fig.6, the fluorescence intensity becomes stronger with the increase of pump power. In addition, a small emission band located at about 1630 nm is observed, corresponding to the $^3H_4 \rightarrow {}^3F_4$ transition of Tm^{3+}, which offer a proof of the improvement of the cross-relaxation energy transfer in our Tm^{3+}-doped PCF.

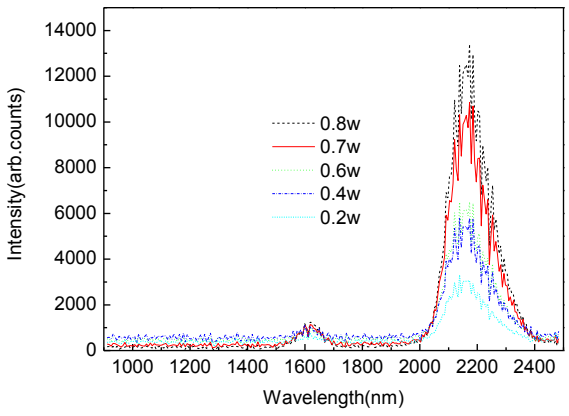

Fig. 6. The fluorescence of Tm^{3+}-doped photonic crystal fiber fabrication by NCVD by using the different power pump.

Based on the above experimental analysis, the successful fabrication of Tm^{3+}-doped PCF with large core with NCVD method will make the fabrication of Tm^{3+}-doped PCF simpler and more convenient. In addition, because this fiber has large doping core, Tm^{3+}-doped PCF will have many applications not only such as high average power fiber laser, high peak power fiber laser operating at 2 μm for materials processing and biomedicine, but also atmospheric propagation, sensing and so on.

4. Conclusion

In summary, the Tm^{3+}-doped silica PCF is successfully fabricated by the NCVD method. The absorption attenuation at 793 nm ($^3H_6 \rightarrow {}^3H_4$) of Tm^{3+}-doped silica PCF can be up to 10.413 dBm^{-1}. An intense broad fluorescence band is located around 2170 nm, corresponding to the $^3F_4 \rightarrow {}^3H_6$ transition of Tm^{3+}. In addition, a small band around 1630 nm corresponds to the $^3H_4 \rightarrow {}^3F_4$ transition of Tm^{3+}, which shows the improvement of the cross-relaxation energy transfer in our Tm^{3+}-doped PCF. The results show that the Tm^{3+}-doped silica PCF may be a preferable candidate for the high power fiber laser around 2 μm.

Acknowledgment

This work was supported by National Natural Science Foundation of China (Grant No 61377100 and 61205084), Guangdong Natural Science Foundation (Grant No S2013040015665), Specialized Research Fund for the Doctoral Program of Higher Education (Grant No 20134407120014) and Colleges and universities in Hebei province science and technology research project (Grant No QN20131044).

References

[1] D. J. Richardson, J. Nilsson, W. A. Clarkson, JOSA B **27**(11), B63 (2010).
[2] L. Andreas, S. Mario, S. Gerhard, G. Stephan, J. Florian, L. Martin, M. Christian, K. Jens; S. Anka, M. Oliver, S. Olaf, N. Roman, W. Björn, R. Georg, K. Volker, SPIE LASE. International Society for Optics and Photonics, Proc. SPIE, 7914, 79150141U (2011).
[3] Y. Jeong, J. Sahu, D. Payne, J. Nilsson, Optics Express **12**(25), 6088 (2004).
[4] R. Zhou, Y. Ju, Y. Zhang, Y. Wang, Chinese Optics Letters **9**(7), 071401 (2011).
[5] P. Zhou, X. Wang, Y. Ma, Z. Liu, Laser Physics **22**(11), 1744 (2012).
[6] A. B. Seddon, Z. Tang, D. Furniss, S. Sujecki, T. M. Benson, Optics Express **18**(25), 26704 (2010).
[7] G. J. Koch, J. Y. Beyon, B. W. Barnes, M. Petros, J. Yu, F. Amzajerdian, M. J. Kavaya, U. N. Singh, Optical Engineering **46**(11), 116201 (2007).
[8] J. P. Cariou, B. Augere, M. Valla, C. R. Physique, Comptes Rendus Physique **7**(2), 213 (2006).
[9] Q. Yi, T. Tsuboi, S. Zhou, Y. Nakai, H. Lin, H. Teng, Chinese Optics Letters **10**(9), 091602 (2012).
[10] O. Kulkarni, V. Alexander, M. Kumar, M. J. Freeman, M. N. Islam, F. L. Terry, M. N. Kandan, A. Chan, JOSA B **28**(10), 2486 (2011).
[11] O. Kulkarni, V. Alexander, M. Kumar, M. N. Islam, M. J. Freeman, F. L. Terry, presented at the Conference on Lasers and Electro-Optics (CLEO), Baltimore, MD, Paper CThD2(2011),
[12] T. S. McComb, R. A Sims, C. C. Willis, P. Kadwani, V. Sudesh, L. Shah, M. Richardson, Applied optics **49**(32), 6236 (2010).
[13] W. A. Clarkson, L. Pearson, Z. Zhang, J. W. Kim, D. Shen, A. J. Boyland, J. K. Sahu, M. Ibsen, In Optical Fiber Communication Conference. Optical Society of America, 2009.
[14] Thomas Ehrenreich, Ryan Leveille, Imtiaz Majid, Kanishka Tankala, Glen Rines and Peter Moulton, SPIE Photonics West 2010: LASE Fiber Lasers VII: Technology, Systems, and Applications, Conference 7580, Session 16: Late-Breaking News, January 28, 2010.
[15] N. Modsching, P. Kadwani, R. A. Sims, L. Leick, J. Broeng, L. Shah, M. Richardson, Optics letters **36**(19), 3873 (2011).
[16] P. K. Kadwani, N. Modshing, R. A. Sims, L. Leick, J. Broeng, L. Shah, M. C. Richardson, Advanced Solid-State Photonics. Optical Society of America, 2012.
[17] C. Gaida, P. Kadwani, L. Leick, J. Broeng, L. Shah, M. Richardson, Opt. Lett. **37**, 4513 (2012).
[18] C. Jollivet, T. T. Alkeskjold, L. Leick, P. Kadwani, R. A. Sims, L. Shah, M. C. Richardson, R. Amezcua Correa, A. Schülzgen, Fiber Lasers and Applications. Optical Society of America, 2012.
[19] C. Gaida, M. Gebhardt, P. Kadwani, L. Leick, J. Broeng, L. Shah, M. Richardson, Opt. Lett. **38**, 97 (2013).
[20] http://en.wikipedia.org/wiki/Sol-gel
[21] S. D. Jackson, Nature Photonics **6**(7), 423 (2012).
[22] M. J. F. Digonnet, Rare-Earth-Doped Fiber Lasers and Amplifiers, Second Edition, Revised and Expanded. (Marcei Dekker Inc., NewYork, USA, 2001), 2nd Chapter.

*Corresponding author: xiacmm@126.com